JOURNAL OF NEUROTRAUMA XX: XXX-XXX (XXXX 00, 2020)

DOI: 10.1089/neu.2019.6975

Original Article

Sodium Cromoglycate Decreases Sensorimotor Impairment and Hippocampal Alterations Induced by Severe Traumatic Brain Injury in Rats

Marysol Segovia-Oropeza,[1] Cindy Santiago-Castañeda,[1] Sandra Adela Orozco-Suárez,[2] Luis Concha,[3] and Luisa Rocha[1]

Abstract

Severe traumatic brain injury (TBI) results in significant functional disturbances in the hippocampus. Studies support that sodium cromoglycate (CG) induces neuroprotective effects. This study focused on investigating the effects of post-TBI subchronic administration of CG on hippocampal hyperexcitability and damage as well as on sensorimotor impairment in rats. In contrast to the control group (Sham+SS group), animals undergoing severe TBI (TBI+SS group) showed sensorimotor dysfunction over the experimental post-TBI period (day 2, 55%, $p < 0.001$; day 23, 39.5%, $p < 0.001$; day 30, 38.6%, $p < 0.01$). On day 30 post-TBI, TBI+SS group showed neuronal hyperexcitability (63.3%, $p < 0.01$). The hippocampus ipsilateral to the injury showed volume reduction (14.4%, $p < 0.001$) with a volume of damage of $0.15 \pm 0.09\ mm^3$. These changes were associated with neuronal loss in the dentate gyrus (ipsilateral, 33%, $p < 0.05$); hilus (ipsilateral, 77%, $p < 0.001$; contralateral, 51%, $p < 0.001$); Cornu Ammonis (CA)1 (ipsilateral, 40%, $p < 0.01$), and CA3 (ipsilateral, 52%, $p < 0.001$; contralateral, 34%, $p < 0.01$). Animals receiving subchronic treatment with CG (50 mg/kg, s.c. daily for 10 days) after TBI (TBI+CG group) displayed a sensorimotor dysfunction less evident than that of the TBI+SS group ($p < 0.001$). Their hippocampal excitability was similar to that of the Sham+SS group ($p = 0.21$). The TBI+CG group presented hippocampal volume reduction (12.7%, $p = 0.94$) and damage ($0.10 \pm 0.03\ mm^3$, $p > 0.99$) similar to the TBI+SS group. However, their hippocampal neuronal preservation was similar to that of the Sham+SS group. These results indicate that CG represents an appropriate and novel pharmacological strategy to reduce the long-term sensorimotor impairment and hippocampal damage and hyperexcitability that result as consequences of severe TBI.

Keywords: hippocampus; hyperexcitability; neuroprotection; sodium cromoglycate; traumatic brain injury

Introduction

Traumatic brain injury (TBI) is a brain insult caused by an external mechanical force to the head, such as an impact, sudden acceleration-deceleration, blast waves, or projectiles.[1] TBI affects ~69,000,000 people worldwide.[2] It is the most important cause of disability and death in young adults worldwide.[3]

Acute events, such as intracranial hemorrhage, neuroinflammation, cerebral edema, excitotoxicity,[4–6] and diffuse neuronal death, take place immediately after TBI.[7,8] Subsequently, a progressive post-traumatic encephalopathy occurs, which is associated with mood disorders,[9] neuromotor damage,[10] neuronal hyperexcitability,[11,12] and neuroendocrine alterations.[13] Currently, it is known that neurodegenerative disorders such as Alzheimer's disease, Parkinson's disease, post-traumatic epilepsy, and stroke can result as long-term consequences of severe TBI.[14] These neurodegenerative disorders represent a significant economic cost. The total direct and indirect costs of TBI in Europe and the United States were estimated in ~ USD $45.4 and $60 billion, respectively.[15,16]

The hippocampus is a brain area susceptible to neuronal damage and hyperexcitability as consequence of a TBI.[11,17–21] The hippocampal alterations following a TBI result in attention, memory, and cognition changes, as well as mood and decision-making ability variations, lack of impulse control, and, eventually, post-traumatic epilepsy.[22] At present, however, no therapeutic strategies exist to avoid long-term consequences of severe TBI in the hippocampus and other brain areas.[23]

Experimental evidence indicates that sodium cromoglycate (CG), a drug that prevents degranulation and migration of mast cells, induces neuroprotective effects.[24,25] In experimental models, CG administration decreases cerebral ischemia effects (neuronal

[1]Department of Pharmacobiology, Center of Research and Advanced Studies, Mexico City, Mexico.
[2]Unit for Medical Research in Neurological Diseases, National Medical Center, Mexico City, Mexico.
[3]Institute of Neurobiology, National Autonomous University of Mexico, Campus Juriquilla, Queretaro, Mexico.

damage, atrophy, and increased astroglial activity) in areas such as the hippocampus, thalamus, and cerebral cortex.[26,27] CG also reduces neuroinflammation, cerebral edema, neuronal damage, neutrophil entry into the brain parenchyma, and mortality resulting from hypoxia and cerebrovascular disorders.[28,29] Previous findings showed that CG pre-treatment delays lithium-pilocarpine-induced *status epilepticus* and reduces subsequent hippocampal damage in rats.[30] Subchronic administration of CG during the post-*status epilepticus* period results in lower frequency and intensity of spontaneous and recurrent seizures and less neuronal damage in the thalamus.[31] This group of evidence supports that CG induces neuroprotective effects in different brain disorders.

The present study focused on investigating if the subchronic administration of CG after a severe TBI could prevent or reduce long-term consequences. Experiments were designed to evaluate sensorimotor functions as well as different hippocampal conditions (excitability, neuronal population, and volume and tissue damage). The results obtained support that CG, a drug of well-known pharmacological characteristics, wide margin of safety, and low cost, is an appropriate pharmacological strategy to prevent or reduce long-term complications resulting from severe TBI.

Methods

Animals

Male Wistar rats (250–300 g) were maintained individually in clear acrylic boxes under controlled environmental conditions (12 h light/darkness cycles, at 22 ± 2°C, and 50% humidity) with access to food and water *ad libitum*.

The experimental protocol was conducted following the Official Mexican Standard (NOM-062-ZOO-1999) and with the approval of the Internal Committee for the Care and Use of Laboratory Animals of the Research and Advanced Studies Center (Mexico, Project 0125-15). All efforts were made to minimize the number of animals used.

Experimental groups

Animals were randomly divided into the following groups.

TBI+CG group ($n = 18$). Under general anesthesia, animals underwent severe TBI. Fourteen rats survived the trauma. Ninety minutes after injury, rats were treated with CG (50 mg/kg, s.c., Sigma-Aldrich), daily for 10 days. CG was applied at 50 mg/kg s.c. because this treatment reduces the neuronal damage subsequent to hypoxic-ischemic events,[26,27] and pilocarpine-induced *status epilepticus*.[30,31]

Thirty days post-TBI, seven rats were anesthetized and perfused. Hippocampal volume and damage were evaluated *ex vivo* using magnetic resonance imaging (MRI). The remaining animals ($n = 7$) were used 23 days post-TBI to evaluate hippocampal excitability and neuronal damage. These rats underwent surgery to implant a bipolar electrode in the ventral hippocampus ipsilateral to the injury. Thirty days post-TBI, their hippocampal excitability was evaluated through the estimation of the after-discharge threshold (ADT). On day 31 post-TBI, rats were anesthetized and perfused. The brain was used to evaluate the neuronal population (NeuN) in different areas of the hippocampus. Weight and sensorimotor function (composite neuroscore [NS]) were evaluated at different time points throughout the experimental procedure (Fig. 1).

TBI+SS group ($n = 18$). Animals underwent the same experimental procedures as the TBI+CG group, except that they received the administration of saline solution (SS) (1 mL/kg; s.c.) instead of CG. Three animals died after the TBI. Eight rats were used for MRI analysis and seven rats were used for histological evaluation (Fig. 1).

Sham+CG group ($n = 10$). This group underwent the same experimental procedures as the TBI+CG group, except for the TBI. Four animals were used for MRI analysis and six for hippocampal assessment (Fig. 1).

Sham+SS group ($n = 15$). Animals underwent the same experimental procedures as the CG group, except for the administration of SS instead of CG. MRI ($n = 8$) and histological evaluation ($n = 7$) were performed (Fig. 1).

Sensorimotor function evaluation

Sensorimotor functions were evaluated with NS.[10,32] NS consists of different tests applied to analyze the following functions: (1) forelimb outstretching, (2) hindlimb outstretching, (3) body lateral pulsion, and (4) balance on an inclined platform. For the first three tests, individual scores were obtained for each of the limbs. A total score of 27–28 indicates a normal condition, a 16–26 score indicates mild damage, and a score of ≤15 indicates severe sensorimotor damage.[33]

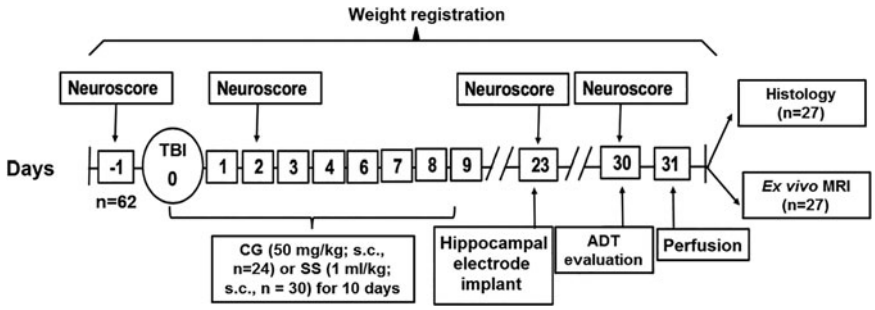

FIG. 1. Timeline of experimental design used to determine the effects of subchronic administration of sodium cromoglycate (CG) after the induction of a severe traumatic brain injury (TBI). Throughout the protocol, the weight of the animals was recorded. Sensorimotor function was evaluated with composite neuroscore (NS) before (-1) and after TBI (days 2, 23, and 30 after trauma). CG or saline (SS) was administered 90 min after the TBI induction and then every 24 h for 10 days. In a group of animals, a bipolar electrode was implanted in the ventral hippocampus on day 23 post-TBI. On day 30 post-TBI, the after-discharge threshold (ADT) was estimated. On day 31, a group of animals was perfused to perform histological analyses, while others were perfused for hippocampal volume and damage assessment by *ex vivo* magnetic resonance imaging (MRI).

Induction of severe TBI

Severe TBI was induced by the lateral fluid-percussion (LFP) injury model according to McIntosh and coworkers.[10] The animals were anesthetized with ketamine, 80 mg/kg, i.p. and xylazine, 15 mg/kg, i.m. (Pisa Labs.). Anesthesia was achieved in most rats 15 min after the injection of the drugs and lasted 20–30 min. Then, animals were sedated for ~3.8, characterized by a period of immobility and reduced responsiveness to external stimuli. During anesthesia, rats were placed in a stereotaxic frame and underwent a sagittal incision followed by a 5 mm diameter craniotomy in the left hemisphere. The center of craniotomy was located according with the following coordinates: anteroposterior relative to Bregma, -3.5 mm; lateral, 3.5 mm. After verifying the integrity of the dura mater, a plastic female Luer-Lock was implanted into the trepan and a stainless steel screw was implanted in the frontal cortex. Both were attached to the skull with dental acrylic. After 90 min of ketamine/xylazine injection, during the sedation period, we confirmed that animals exhibited a toe pinch response. Then, they were connected through the Luer-Lock to a radius angled tip of 90 degrees attached to a fluid-percussion brain damage device (AmScience Instruments, Richmond, VA, USA), and severe TBI was induced by applying a pressure of 2.6–3.3 atm.[34] At the end of the procedure, the implant was removed, the wound was closed, and tramadol (20 mg/kg, s.c., NorVet) was administered.

Electrode implantation and assessment of hippocampal excitability

Rats previously anesthetized (ketamine, 80 mg/kg, i.p.; xylazine, 15 mg/kg, i.m.) were placed in a stereotaxic frame. A bipolar electrode was implanted in the ventral hippocampus (anteroposterior, -5.3 mm in relation to Bregma; lateral, 5.2 mm; height, 7.5 mm), ipsilateral to the injury.[35] Three stainless steel screws were placed on the skull to support the implant, which was fixed with dental acrylic. ADT was estimated 7 days after surgery. The procedure consisted of the application of a train of electrical stimuli (1 ms square pulses at 60 Hz for 1 sec) generated with a GRASS S-48 model stimulator. The procedure was repeated every minute with an initial electric current of 10 μA, which was subsequently increased by 20% until a behavioral change or an electrographic after-discharge was induced.[36] Low values indicate neuronal hyperexcitability.

Histology and fractional counting method

Under anesthesia (ketamine, 80 mg/kg, i.p.; xylazine, 15 mg/kg, i.m.), animals were perfused with 250 mL of SS (0.9%) and heparin (1 mg/L, Sigma-Aldrich, Cat # H3393), followed by 250 mL of paraformaldehyde (4%, Sigma-Aldrich Cat # P6148) and glutaraldehyde (0.2%, Electron Microscopy Sci. Cat # 16210) in a phosphate buffer solution (PBS). After perfusion, the brain was dissected and kept in a paraformaldehyde solution (4%, Sigma-Aldrich Cat # P6148) at 4°C for 168 h. Subsequently, it was included in paraffin for further processing. Brains were sectioned (5 μm thickness each section) in the coronal plane. Serial sections (1 of 5) through the entire dorsal hippocampus (Bregma -2.5 to -4.5 mm) were collected and thaw-mounted on Poly-L-lysine adhesive (Sigma-Aldrich Cat # P8920) coated glass slides.

Brain sections were used to evaluate NeuN, a neural marker, by immunohistochemistry. For this procedure, brain sections were first incubated in an antigenic recovery solution (Diva, Biocare Medical) (10 min at 120°C), and then washed in distilled water and exposed to H_2O_2 at 3% (10 min). Then, sections were incubated in goat serum (1:200, 30 min, Vector Lab USA) and subsequently in the primary mouse monoclonal antibody directed against NeuN (1:200, 72 h, Millipore Cat # MAB-377). Brain sections were then incubated with the secondary antibody (anti-mouse peroxidase) (1:200, 2 h, Vector Lab. Cat # PI-200). Finally, the reaction was revealed with 3,3'-diaminobenzidine tetrahydrochloride (Betazoid DAB Chromogen Kit, Biocare Medical Cat # kit DB801L). The slides with the brain sections were covered with synthetic resin (Entellan®, Merck Millipore). Digitized images of the brain sections were obtained with a camera connected to a microscope (Nikon 10x Optical 200M) and analyzed using the Image Pro-Plus 7 processing software (Media Cybernetics, USA).

The fractional counting method by West and coworkers[37] was used for the estimation of the number of neurons per volume (mm^3) in different regions of the hippocampus: dentate gyrus (DG), hilus, Cornu Ammonis (CA)1, and CA3, ipsi- and contralateral to injury or manipulation. One investigator performed this procedure under blind conditions. The regions of interest were identified at the level of dorsal hippocampus (Bregma -2.5 to -3.6 mm) on digital images previously obtained with a light microscope (Eclipse Ni; Nikon, Japan) and Image Pro-Plus 7 software (Media Cybernetics, USA). Three serial sections obtained at intervals of every fifth section (see *Histology* section) were evaluated for this purpose. In this case, the sampling fraction (*ssf*) corresponded to 1/5. The area sampling fraction (*asf*) = area (frame)/area (x, y step) was calculated and corresponded to the counting frame (0.460 × 0.600 mm). Then, the thickness sampling fraction was estimated with the dissector height (*h*) relative to the section thickness *t* (*h/t*). The number of cells was calculated using the following formula: $N = (\sum Q^-)$ x (*t/h*) x (*1/asf*) x (*1/ssf*). In this formula, Q^- represented the number of cells in a known volume fraction of each area evaluated.

Ex vivo MRI

The perfusion protocol was conducted as previously described for the histological evaluation, with the difference that gadolinium-based contrast agent (2 mM, Prohance, Bracco Diagnostics Inc.) was added to the solution.[38] At the end of the perfusion, the animal's head was removed from the body and immersed in paraformaldehyde (4%) and ProHance (2 mM) at 4°C overnight. The following day sodium azide (Sigma-Aldrich Cat # S2002) was added (0.02%) to the buffer. The samples were stored at 4°C until imaging.

Imaging was performed at the National Laboratory for MRI (UNAM) using a Bruker Pharmascan 70/16 US 7.0 T magnet and a circularly polarized rat head coil, coupled to a workstation running Paravision 6.0.1. The procedure was performed at room temperature (21 ± 1°C). The parameters for the scans were optimized for gray- and white-matter contrast (Fast Low Angle Shot [FLASH] imaging with three-dimensional [3D] acquisition). The resolution was 85 μm per side (repetition time [TR]/echo time [TE]/flip angle = 30 ms/8.6 ms/20 degrees). The acquisition time per animal was 1 h. Volumes were linearly normalized to a custom-made, unbiased, rat brain atlas. Said atlas was built by interactively registering all image volumes using a non-linear transform,[39] using the Wazholm Space atlas of the Sprague Dawley rat brain[40] as a starting point. The total volume of each hippocampus was calculated by manually selecting the areas of interest, using as a reference an atlas of the rat brain[35] and the ITK-SNAP software version 3.6.0.[41] Similarly, areas corresponding to damage (hypointense voxels) were selected, and the total volumes of hippocampal injury were obtained. Brains that showed image alterations under control conditions were discarded.

Statistical analysis

Each of the procedures was performed by a researcher blind to the experimental conditions. A two-way analysis of variance (ANOVA) followed by a Tukey *post-hoc* test was used to compare the obtained values. For non-parametric values, the Kruskal–Wallis test, followed by a Dunn *post-hoc* was used. Data were expressed as

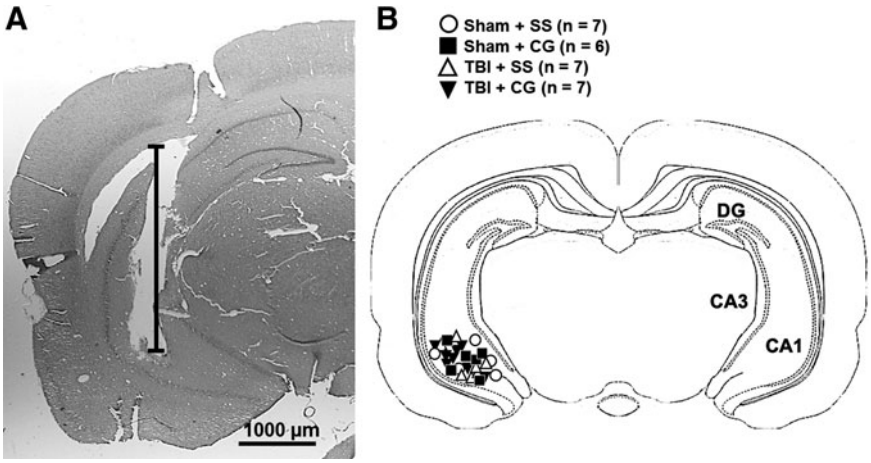

FIG. 2. **(A)** Representative microphotograph of a coronal section labeled with Nissl staining showing the area of electrode implantation in the ventral hippocampus. The black line indicates the placement of the bipolar electrode implantation. **(B)** A diagram at -5.28 mm from Bregma (modified from Paxinos and Watson[35]), indicating the places where the electrode tips were implanted in the ventral hippocampus of animals of the different experimental groups used for after-discharge estimation.

a mean ± standard error (SE). A value of $p < 0.05$ was considered statistically significant. Data were analyzed with GraphPad Prism version 7.0 for Mac OS X (GraphPad Software, San Diego, CA, USA).

Results

In the present study, histological analysis showed that electrode tips were implanted within the left ventral hippocampus in all of the rats used (Fig. 2).

Animals from the Sham+SS group presented body weight of 251 ± 3 g at the beginning of the experiments, and 384.4 ± 5 g when the procedures ended (Fig. 3). Throughout the experimental procedures, their sensorimotor activity was normal, with a score of 27–28 evaluated with NS (Fig. 4). ADT was achieved with 384.3 ± 18.09 μA (Fig. 5).

Ex vivo MRI analysis of the Sham+SS group revealed hippocampal volumes of 54.8 ± 0.69 and 55.6 ± 1 mm^3, ipsi- and contralateral to craniotomy, respectively. Hippocampal damage was not detected (Table 1 and Supplementary Figures). The stereological analysis showed no differences in the number of NeuN positive cells per mm^3 in the hippocampus, ipsi- and contralateral to craniotomy (Table 2, Fig. 6).

No statistical differences were observed in the results obtained from the Sham+CG group, when compared with those from the Sham+SS group (Figs. 3–6; Tables 1 and 2; Supplementary Figures).

The animals of the TBI+SS group received a fluid percussion injury of 3.084 ± 0.11 atm to induce a severe TBI. They showed a decrease in their body weight of up to 12% ($p < 0.001$) during the first 6 days after TBI. Thereafter, rats showed a progressive weight recovery throughout the experimental period, although the values remained lower in comparison with the Sham+SS group (Fig. 3). Regarding the sensorimotor function, the TBI+SS group presented significantly lower values than the Sham+SS group (day 2 post-TBI, 55%, $p < 0.001$; day 23 post-TBI, 39.5%, $p < 0.001$; day 30 post-TBI, 38.6%, $p < 0.01$) (Fig. 4). TBI+SS group showed lower ADT values than the Sham+SS group (63.3%; $p < 0.01$) (Fig. 5), indicating hippocampal hyperexcitability.

In comparison with the Sham+SS group, the TBI+SS group showed a lower hippocampal volume (14.4%) ipsilateral to the injury ($p < 0.001$), with a volume of damage of 0.15 ± 0.09 mm^3. The contralateral hippocampus showed no volume changes ($p > 0.05$) or evidence of damage (Table 1 and Supplementary Figures).

Concerning the histological assessment, the TBI+SS group showed a decrease in neuronal survival in the hippocampal areas evaluated. This effect was statistically significant for the ipsilateral DG (66%, $p < 0.05$); ipsilateral (22%, $p < 0.001$) and contralateral hilus (48%, $p < 0.001$); ipsilateral CA1 (60%, $p < 0.01$); and ipsilateral (47%, $p < 0.001$) and contralateral CA3 (66%, $p < 0.01$), when compared with the Sham+SS group (Table 2, Fig. 6).

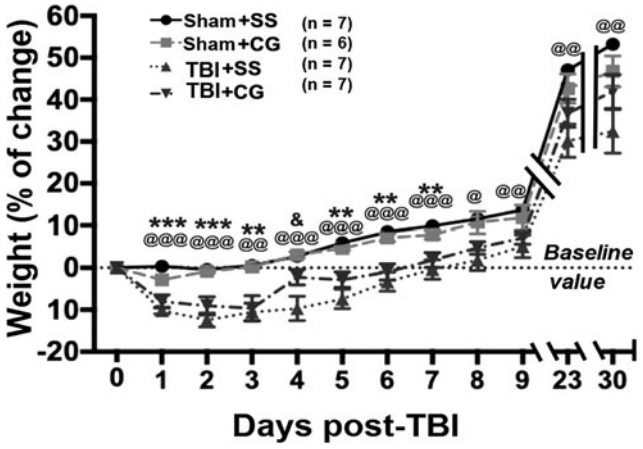

FIG. 3. Effects of sodium cromoglycate (CG) on body weight alterations secondary to a severe traumatic brain injury (TBI). The graph shows the representation of body weight changes in the different groups throughout the experimental procedure. Sham+SS and Sham+CG groups showed a progressive increase in body weight. Conversely, the TBI+SS group presented a weight decrease after the 1st day post-TBI. Thereafter, these animals showed a progressive increase in body weight, but never achieved the values of the Sham+SS group. A similar evolution was observed in the TBI+CG group. The values represent the mean ± standard error (SE) of the percentage of weight change relative to baseline values (day 0). $^{@}p < 0.05$, $^{@@}p < 0.01$, $^{@@@}p < 0.001$ (TBI+SS vs. Sham+SS); $^{**}p < 0.01$, $^{***}p < 0.001$ (TBI+CG vs. Sham+SS); $^{\&}p < 0.05$ (TBI+CG vs. TBI+SS). SS, saline.

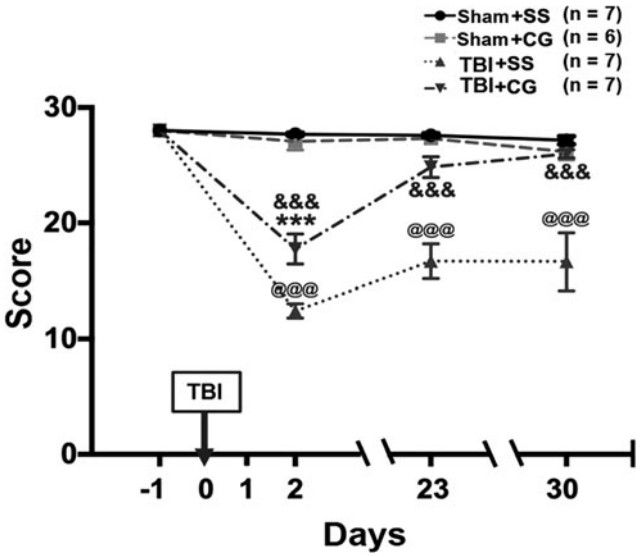

FIG. 4. Representation of the composite neuroscore (NS) values during the experimental procedure. Animals from the Sham+SS and Sham+CG groups maintained an NS rate of 27–28 throughout the different evaluations. In contrast, the TBI+SS group presented a significant decrease at 24 h and 23 and 30 days after traumatic brain injury (TBI). The TBI+CG group also showed a decrease in sensorimotor function. However, it was less evident when compared with the TBI+SS group, and achieved basal levels 30 days post-TBI. The values represent the mean ± standard error (SE) of the scores obtained in the NS evaluations. $^{@@@}p < 0.001$ (TBI+SS vs. Sham+SS); $^{***}p < 0.001$ (TBI+CG vs. Sham+SS); $^{\&\&\&}p < 0.001$ (TBI+CG vs. TBI+SS). CG, sodium cromoglycate; SS, saline.

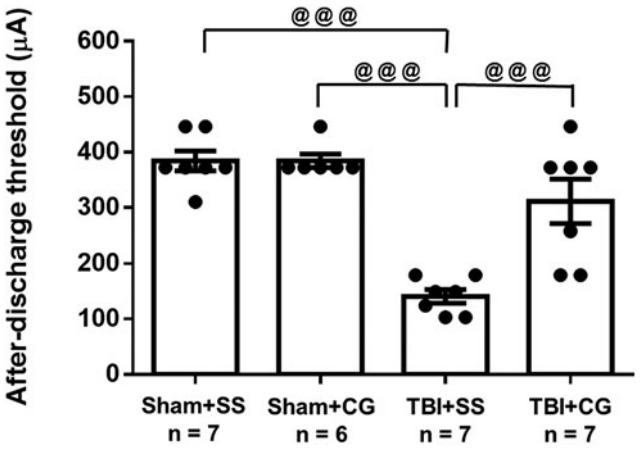

FIG. 5. Effects of sodium cromoglycate (CG) on traumatic brain injury (TBI)-induced hippocampal excitability alterations estimated by the after-discharge threshold (ADT). Sham+SS and Sham+CG groups showed similar ADT values. However, the TBI+SS group showed significantly lower values than both the Sham+SS and Sham+CG groups, indicating hippocampal hyperexcitability. The TBI+CG group showed higher values than the TBI+SS group, which indicates less excitability. Values are expressed as the mean ± standard error (SE) of the μA required to achieve the ADT. $^{@@@}p < 0.001$ vs. TBI+SS. SS, saline.

TABLE 1. VOLUME OF HIPPOCAMPUS AND LESIONS, IPSILATERAL OR CONTRALATERAL TO INJURY ASSESSED WITH *EX VIVO* MAGNETIC RESONANCE IMAGING

	Hippocampus volume (mm^3)		*Volume of injury (mm^3)*	
Group	*Ipsilateral*	*Contralateral*	*Ipsilateral*	*Contralateral*
Sham+SS ($n=8$)	54.83±0.69	55.67±1	0	0
Sham+CG ($n=4$)	51.5±1	52.9±1.1	0	0
TBI+SS ($n=8$)	46.92± 0.9***	53.14±1.3	0.15± 0.09**	0
TBI+CG ($n=6$)	47.86± 1.93***	53.96±1.7	0.10± 0.03**	0

Data represent mean ± SE in mm^3.
$^{**}p < 0.01$; $^{***}p < 0.001$ versus Sham + SS.
SS, saline solution; CG, cromoglycate; TBI, traumatic brain injury; SE, standard error.

In the TBI+CG group, a severe TBI was induced applying a fluid percussion injury of 3.047 ± 0.12 atm ($p = 0.8304$ vs. the TBI+SS group). As result of the trauma, the TBI+CG group showed a weight loss similar to that exhibited by the TBI+SS group (Fig. 3). The NS indicated a decrease in sensorimotor function following TBI (day 2, 36%, $p < 0.001$; day 23, 11%, $p < 0.02$; day 30, 7%, $p > 0.05$, in comparison with baseline values). However, in this group, sensorimotor dysfunction was less evident than in the TBI+SS group ($p < 0.001$, Fig. 4). For the ADT evaluation, the values obtained were similar to those of the Sham+SS group ($p = 0.21$) (Fig. 5).

One animal was not included in the MRI analysis because the brain was bloody after perfusion. The hippocampal volume and volume of damage in six rats of the TBI+CG group were similar to those in the TBI+SS group (volume, 12.7%, $p = 0.94$; damage, 0.10 ± 0.03 mm^3, $p > 0.99$) (Table 1 and Supplementary Figures). Finally, the histological analysis showed neuronal preservation similar to the Sham+SS group in the different hippocampal areas evaluated (Table 2, Fig. 6).

Discussion

CG is a mast cell stabilizer of known pharmacological characteristics and a wide safety margin.[24,25] CG exerts its neuroprotective effects by preventing the release of several factors contained in the granules of mast cells, which favor tissue damage: amines, proinflammatory cytokines, tissue-degrading enzymes, prostaglandins, reactive oxygen species, and histamine.[42] The results obtained from this study show for the first time that CG administration reduces the deterioration in sensorimotor functions resulting from severe TBI. Also, post-TBI hippocampal hyperexcitability is less evident, an effect associated with reduced neuronal and brain damage. However, CG subchronic administration prevent neither body weight loss nor hippocampal volume decrease secondary to severe TBI.

CG is a highly polar compound, which is poorly absorbed from the gastrointestinal tract (< 4%).[43] It is not metabolized and after i.v. administration, it is cleared rapidly by both renal and hepatic excretion with a plasma half-life of 20 min in rats.[44] After subcutaneous administration, CG clearance is 43.9 mL/min/kg in adult rats, and very low levels are detected at 24 h (< 0.001% of total dose).[45] In rats, the chronic CG administration at 200 mg/kg; s.c.

Table 2. Number of NeuN Positive Cells in Areas of the Dorsal Hippocampus, Ipsilateral or Contralateral to TBI or Craniotomy in the Experimental Groups

	Dentate gyrus		*Hilus*		*CA1*		*CA3*	
Group	*Ipsi-*	*Contra-*	*Ipsi-*	*Contra-*	*Ipsi-*	*Contra-*	*Ipsi-*	*Contra-*
Sham+SS ($n=7$)	3316±292	3659±313	513±26	421±33	1775±133	1659±138	1132±82	1150±61
Sham+CG ($n=6$)	3120±105	3617±373	473±59	443±40	1854±62	1823±84	943±59	1117±88
TBI+SS ($n=7$)	2217±168*	2887±268	114±12***	202±24***	1062±68**	1332±141	536±76***	757±69**
TBI+CG ($n=7$)	2993±300	3628±241	457±13	453±28	1762±183	1705±113	1065±98	1118±93

Data are presented as the mean ± SE of neural preservation (mm^3). ipsilateral (ipsi-) or contralateral (contra-) to the injury site.
*$p<0.05$; **$p<0.01$; ***$p<0.001$ versus Sham+SS.
SS, saline solution; CG, sodium cromoglycate; TBI, traumatic brain injury; SE, standard error.

induces toxic effects that result in renal damage and a mortality rate of 4%.[46] A previous study suggested that CG does not cross the blood–brain barrier.[46] However, several publications support its therapeutic efficacy as a mast cell stabilizer in the brain when administered i.v. or s.c.[29–31,47]

It has been reported that the administration of CG promotes body weight gain because of an increase in food and water intake in experimental models of hypophagia.[48,49] This effect is explained because CG prevents mast cell degranulation with a subsequent decrease in histamine levels, as well as the activation of the H1 receptor in the ventromedial and paraventricular nucleus, which regulate food intake.[50] In this study, animals undergoing severe TBI showed a decrease in body weight, consistent with studies in other animal models,[51,52] as well as in humans.[53] However, the repeated administration of CG did not prevent post-TBI weight loss. TBI may affect brain areas such as the hypothalamus, which favors weight loss by hypermetabolism,[52] a condition that was not modified with the CG subchronic treatment.

Sensorimotor functions regulated by the cerebral cortex are known to be affected after the first hours after a TBI. This condition can remain over the long-term following severe trauma.[10,33,54] The present results demonstrate that animals receiving subchronic CG treatment after severe TBI show lower sensorimotor dysfunction, which was reversed within 30 days post-trauma. This effect is similar to that reported by other authors, who described that CG pre-treatment promotes neurological and motor recovery in experimental models of brain hemorrhage.[29] It is possible to suggest that the stabilization of mast cells by CG may prevent the release of pro-inflammatory factors and the subsequent cell damage at the level of the sensorimotor cortex.

In the present study, histology was performed in the dorsal hippocampus, because this brain area shows higher cell loss as a

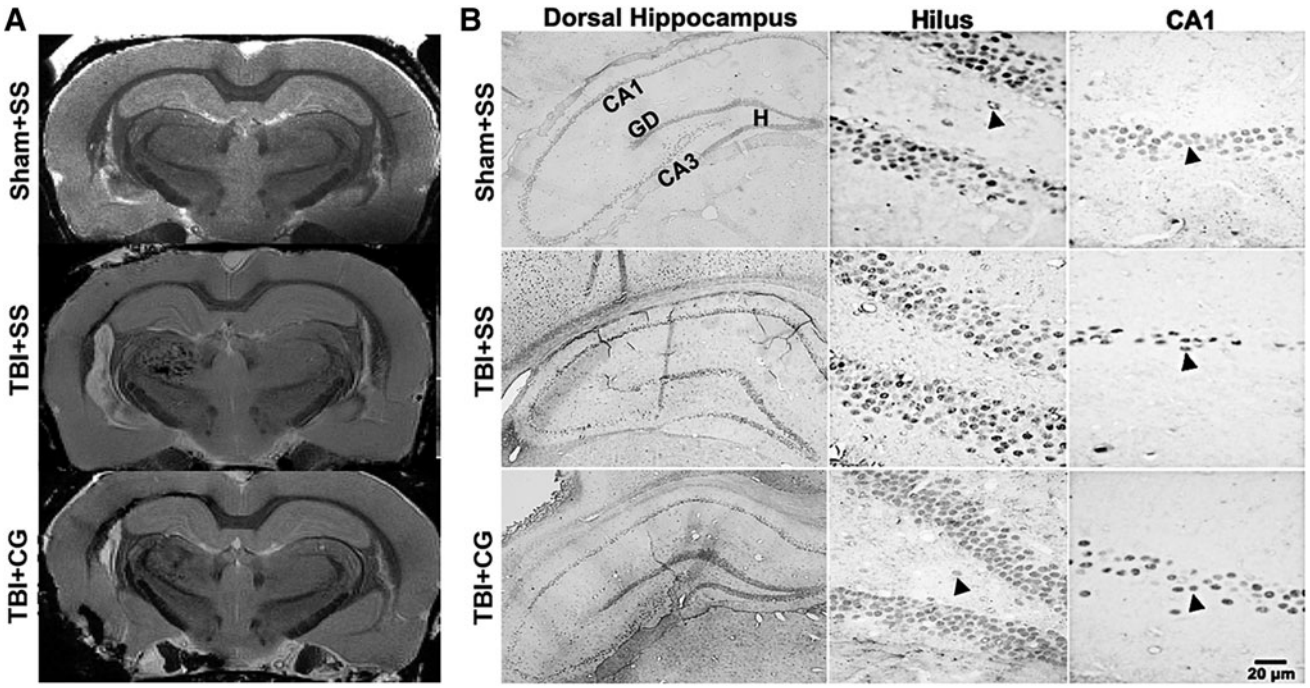

FIG. 6. Effects of subchronic treatment with sodium cromoglycate (CG) on hippocampal damage subsequent to a severe traumatic brain injury (TBI). **(A)** Representative coronal images of *ex vivo* magnetic resonance imaging (MRI) with T2 contrast at the level of the dorsal hippocampus from Sham+SS, TBI+SS, and TBI+CG groups. **(B)** Microphotographs obtained from immunohistochemistry experiments for neuronal population (NeuN) in the dorsal hilus and Cornu Ammonis (CA)1 of the Sham+SS, TBI+SS, and TBI+CG groups. A lower number of immunoreactive cells in the TBI+SS group than in the Sham+SS group is noticeable. This change was unnoticeable in the TBI+CG group. H, hilus; DG, dentate gyrus; SS, saline.

consequence of TBI, in contrast to the ventral hippocampus.[55] The histological assessment of the TBI+SS group revealed a decrease in neuronal survival in the different dorsal hippocampal areas evaluated. Concerning severe TBI in rats, Grady and coworkers[56] found cell loss in hippocampus ipsilateral to the trauma at 2 weeks after a severe TBI as follows: hilus, 50%; CA1, 13%; CA3, 22%. In the present study, the results obtained revealed a higher cell loss 1 month after a severe TBI in rats (DG, 33%; hilus, 77%; CA1, 40%; CA3, 52%, ipsilateral to trauma). This group of evidence supports the progression of cell damage after a severe TBI. In contrast to our results, Baldwin and coworkers[57] reported less cell loss in CA3 (40%) 1 month after a severe TBI. This discrepancy can be explained because we used a fluid-percussion device equipped with an angled tip, instead of a straight one as used by other authors.[58,59] In this model, this variation can modify the direction and extent of brain deformation and cause a significant difference in the severity of tissue damage.[60] Other variation is the intensity of the trauma. In contrast to the results obtained in animals with severe TBI (present study,[56,57]) a moderate TBI induces less cell loss in the hippocampus of rodents, 1 week (DG, 44%; hilus, 34%; CA1, 32%; CA3, 32%),[61] and 2 months after TBI (hilus, 40%).[62,63] The discrepancy in the results of cell loss can also be associated with different sectioning planes and definition of the areas of interest established for the stereological procedure used. In addition, the administration of anesthetic/sedative agents can modify the neuronal death induced by TBI. Regarding this issue, it is described that ketamine, the anesthetic used in the present study, is associated with a high hippocampal cell loss after TBI in rats.[64]

Ex vivo MRI and histology results support that injury induces hippocampal damage and decreases the volume of the hippocampus ipsilateral to TBI after the first hours after trauma.[62,63,65] Hippocampal volume reduction secondary to TBI is explained by the significant loss of synapses and other elements in the neuropil.[66,67] Particularly, it is known that a severe TBI results in a decrease of the neuronal population in the DG, hilus, CA1, and CA3.[62,63,65,68] The results obtained indicate that post-TBI subchronic treatment with CG prevented neuronal loss in different hippocampal areas, which is consistent with the neuroprotective effects induced by this drug in other models of brain injury, such as cerebral hemorrhage, hypoxia-ischemia, rotenone damage, and *status epilepticus*.[26–28,30,31,69] However, *ex vivo* MRI results indicate that CG subchronic administration did not prevent the reduction of hippocampal volume ipsilateral to the injury. Such treatment may favor hippocampal neuronal survival, although it does not prevent changes induced by TBI in other cellular components involved in the volume of brain structures.[70]

It is known that severe TBI may result in hippocampal hyperexcitability.[18,19,71] Brain hyperexcitability secondary to TBI has been evaluated by the systemic administration of subconvulsant doses of excitatory drugs such as pentylenetetrazol.[72] However, this experimental strategy does not allow determination of changes in specific brain areas such as the hippocampus. In this study, the estimation of ADT in freely moving animals confirmed that TBI induces hyperexcitability (low ADT values) in the ventral hippocampus, an area with high sensitivity to electrical stimulation.[71,72] Post-TBI hippocampal hyperexcitability is explained as consequence of cell loss and the establishment of hyperexcitable aberrant circuitry.[73–76] It is expected that TBI-induced hyperexcitability in the ventral hippocampus could be associated with functional alterations developed as consequence of a severe TBI.[77] The results obtained from the present study revealed that subchronic treatment of CG after severe TBI prevents changes in hippocampal excitability, which is associated with lower neuronal damage observed by histological evaluation.

This study concludes that CG represents a neuroprotective strategy to prevent or diminish the long-term consequences of severe TBI. However, further studies are necessary to investigate if CG administration is able to prevent the behavioral and cognitive changes induced by severe TBI. It is also important to augment the CG-induced neuroprotective effects. For example, it would be interesting to analyze other types of administration (e.g., continuous infusion with osmotic pumps) as well as the combination of CG with other drugs.

Acknowledgment

The authors acknowledge the technical support of Dr. Juan Ortiz during the MRI experiments.

Funding Information

This study was supported by the National Council for Sciences and Technology of Mexico (CONACYT Scholarship number 458195).

Author Disclosure Statement

No competing financial interests exist.

Supplementary Material

Supplementary Figures

References

1. Pitkänen, A., and Bolkvadze, T. (2012). *Head trauma and epilepsy, in: Jasper's Basic Mechanisms of the Epilepsies*. 4th ed. J.L. Noebels, M. Avoli, M.A. Rogawski, R.W. Olsen, and A.V. Delgado-Escueta (eds.). National Center for Biotechnology Information: Bethesda, MD, pp. 331–342.
2. Dewan, M.C., Rattani, A., Gupta, S., Baticulon, R.E., Hung, Y., Punchak, M., Agrawal, A., Adeleye, A.O., Shrime, M.G., Rubiano, A.M., Rosenfeld, J.V., and Park, K. B. (2018). Estimating the global incidence of traumatic brain injury. J. Neurosurg. 130, 1080–1097.
3. CENTER-TBI. (2020). CENTER-TBI. http://www.center-tbi.eu/ (Last accessed December 17, 2019)
4. Faden, A.I., Demediuk, P., Panter, S.S., and Vink, R. (1989). The role of excitatory amino acids and NMDA receptors in traumatic brain injury. Science 244, 798–800.
5. Purves, D., Augustine, G.J., Fitzpatrick, D., Hall, W.C., LaMantia, A.S., McNamara, J.O., and Williams, S.M. (eds.). (2004). *Neuroscience,* 3rd ed. Sinauer Associates: Sunderland, MA.
6. Morganti-Kossmann, M.C., Satgunaseelan, L., Bye, N., and Kossmann, T. (2007). Modulation of immune response by head injury. Injury 38, 1392–1400.
7. Conti, A.C., Raghupathi, R., Trojanowski, J.Q., and McIntosh, T.K. (1998). Experimental brain injury induces regionally distinct apoptosis during the acute and delayed post-traumatic period. J. Neurosci. 18, 5663–5672.
8. Sato, M., Chang, E., Igarashi, T., and Noble, L.J. (2001). Neuronal injury and loss after traumatic brain injury: time course and regional variability. Brain Res. 917, 45–54.
9. Kim, E., Lauterbach, E.C., Reeve, A., Arciniegas, D.B., Coburn, K.L., Mendez, M.F., Rummans, T.A., and Coffey, E.C. (2007). Neuropsychiatric complications of traumatic brain injury: a critical review of the literature (a report by the ANPA Committee on Research). J. Neuropsychiatry Clin. Neurosci. 19, 106–127.
10. McIntosh, T.K., Vink, R., Noble, L., Yamakami, I., Fernyak, S., Soares, H., and Faden, A.L. (1989). Traumatic brain injury in the rat: characterization of a lateral fluid-percussion model. Neuroscience 28, 233–244.
11. Akasu, T., Muraoka, N., and Hasuo, H. (2002). Hyperexcitability of hippocampal CA1 neurons after fluid percussion injury of the rat cerebral cortex. Neurosci. Lett. 329, 305–308.

12. Griesemer, D., and Mautes, A.M. (2007). Closed head injury causes hyperexcitability in rat hippocampal CA1 but not in CA3 pyramidal cells. J. Neurotrauma 24, 1823–1832.
13. Krahulik, D., Zapletalova, J., Frysak, Z., and Vaverka, M. (2010). Dysfunction of hypothalamic–hypophysial axis after traumatic brain injury in adults. J. Neurosurg. 113, 581–584.
14. Wilson, L., Stewart, W., Dams-O'Connor, K., Diaz-Arrastia, R., Horton, L., Menon, D.K., and Polinder, S. (2017). The chronic and evolving neurological consequences of traumatic brain injury. Lancet Neurol. 16, 813–825.
15. Finkelstein, E.A., Corso, P.S. and Miller, T.R. (2006). *The Incidence and Economic Burden of Injuries in the United States*. Oxford University Press: New York.
16. Olesen, J., Gustavsson, A., Svensson, M., Wittchen, H.U., Jönsson B, CDBE2010 Study Group, and European Brain Council (2012). The economic cost of brain disorders in Europe. Eur. J. Neurol. 19, 155–162.
17. Swartz, B.E., Houser, C.R., Tomiyasu, U., Walsh, G.O., DeSalles, A., Rich, J.R., and Delgado-Escueta, A. (2006). Hippocampal cell loss in posttraumatic human epilepsy. Epilepsia 47, 1373–1382.
18. Santhakumar, V., Bender, R., Frotscher, M., Ross, S.T., Hollrigel, G.S., Toth, Z., and Soltesz, I. (2000). Granule cell hyperexcitability in the early post-traumatic rat dentate gyrus: the 'irritable mossy cell' hypothesis. J. Physiol. 524(Pt 1), 117–134.
19. Santhakumar, V., Ratzliff, A.D., Jeng, J., Toth, Z., and Soltesz, I. (2001). Long-term hyperexcitability in the hippocampus after experimental head trauma. Ann. Neurol. 50, 708–717.
20. Grady, M.S., Charleston, J.S., Maris, D., Witgen, B.M., and Lifshitz, J. (2003). Neuronal and glial cell number in the hippocampus after experimental traumatic brain injury: analysis by stereological estimation. J. Neurotrauma 20, 929–941.
21. Golarai, G., Greenwood, A.C., Feeney, D.M., and Connor, J.A. (2001). Physiological and structural evidence for hippocampal involvement in persistent seizure susceptibility after traumatic brain injury. J. Neurosci. 21, 8523–8537.
22. Ozga, J.E., Povroznik, J.M., Engler-Chiurazzi, E.B., and Vonder Haar C. (2018). Executive dysfunction after traumatic brain injury: special considerations for behavioral pharmacology. Behav. Pharmacol. 29, 617–637.
23. Chew, E., and Zafonte, R.D. (2009). Pharmacological management of neurobehavioral disorders following traumatic brain injury—a state-of-the-art review. J. Rehabil. Res. Dev. 46, 851–879.
24. Howell, J.B., and Altounyan, R.E. (1967). A double-blind trial of disodium cromoglycate in the treatment of allergic bronchial asthma. Lancet 2, 539–542.
25. Kusner, E.J., Dubnick, B., and Herzing, D.J. (1973). The inhibition by disodium cromoglycate in vitro of anaphylactically induced histamine release from rat peritoneal mast cells. J. Pharmacol. Exp. Ther. 184, 41–46.
26. Jin, Y., Silverman, A.J., and Vannucci, S.J. (2007). Mast cell stabilization limits hypoxic-ischemic brain damage in the immature rat. Dev. Neurosci. 29, 373–384.
27. Jin, Y., Silverman, A.J., and Vannucci, S.J. (2009). Mast cells are early responders after hypoxia-ischemia in immature rat brain. Stroke 40, 3107–3112.
28. Strbian, D., Karjalainen-Lindsberg, M.L., Tatlisumak, T., and Lindsberg, P.J. (2006). Cerebral mast cells regulate early ischemic brain swelling and neutrophil accumulation. J. Cereb. Blood Flow Metab. 26, 605–612.
29. Strbian, D., Karjalainen-Lindsberg, M.L., Kovanen, P.T., Tatlisumak, T., and Lindsberg, P.J. (2007). Mast cell stabilization reduces hemorrhage formation and mortality after administration of thrombolytics in experimental ischemic stroke. Circulation 116, 411–418.
30. Valle-Dorado, M.G., Santana-Gómez, C.E, Orozco-Suárez, S.A., and Rocha, L. (2015). The mast cell stabilizer sodium cromoglycate reduces histamine release and status epilepticus-induced neuronal damage in the rat hippocampus. Neuropharmacology 92, 49–55.
31. Valle-Dorado, M.G., Santana-Gómez, C.E, Orozco-Suárez, S.A., and Rocha, L. (2018). Sodium cromoglycate reduces short- and long-term consequences of status epilepticus in rats. Epilepsy Behav. 87, 200–206.
32. Thompson, H.J., Lifshitz, J., Marklund, N., Grady, M.S., Graham, D.I., Hovda, D.A., and McIntosh, T.K. (2005). Lateral fluid percussion brain injury: a 15-year review and evaluation. J. Neurotrauma 22, 42–75.
33. Pierce, J.E., Smith, D.H., Trojanowski, J.Q., and McIntosh, T.K. (1998). Enduring cognitive, neurobehavioral and histopathological changes persist for up to one year following severe experimental brain injury in rats. Neuroscience 87, 359–369.
34. Immonen, R.J., Kharatishvili, I., Gröhn, H., Pitkänen, A., and Gröhn, O.H.J. (2009). Quantitative MRI predicts long-term structural and functional outcome after experimental traumatic brain injury. NeuroImage 45, 1–9.
35. Paxinos, G., and Watson, C. (2007). *The Rat Brain in Stereotaxic Coordinates*. Academic Press: Amsterdam.
36. Racine, R.J. (1972). Modification of seizure activity by electrical stimulation. II. 103 Motor seizure. Electroencephalogr. Clin. Neurophysiol. 32, 281–294.
37. West, M.J., Slomianka, L., and Gundersen, H.J.G. (1991). Unbiased stereological estimation of the total number of neurons in the subdivisions of the rat hippocampus using the optical fractionator. Anat. Rec. 231, 482–497.
38. Ellegood, J., Pacey, L.K., Hampson, D.R., Lerch, J.P., and Henkelman, R.M. (2010), Anatomical phenotyping in a mouse model of fragile X syndrome with magnetic resonance imaging. Neuroimage 53, 1023–1029.
39. Avants, B.B., Tustison, N.J., Song, G., Cook, P.A., Klein, A., and Gee, J.C. (2011). A reproducible evaluation of ANTs similarity metric performance in brain image registration. Neuroimage 54, 2033–2044.
40. Papp, E.A., Leergaard, T.B., Calabrese, E., Johnson, G.A., and Bjaalie, J.G. (2014). Waxholm space atlas of the Sprague Dawley rat brain. NeuroImage 97, 374–386
41. Yushkevich, P.A., Pashchinskiy, A., Oguz, I., Mohan, S., Schmitt, J.E., Stein, J.M., Zukić, D., Vicory, J., McCormick, M., Yushkevich, N., Schwartz, N., Gao, Y., and Gerig, G. (2019). User-guided segmentation of multi-modality medical imaging datasets with ITK-SNAP. Neuroinformatics 17, 83–102.
42. Da Silva, E.Z., Jamur, M.C., and Oliver, C. (2014) Mast cell function: a new vision of an old cell. J. Histochem. Cytochem. 62, 698–738.
43. Moss, G. F., and Ritchie, J. T. (1970). The absorption and clearance of disodium cromoglycate from the lung in rat, rabbit and monkey. Toxicol. Appl. Pharmacol. 17, 699–670.
44. Ashton, M.J., Clark, B., Jones, K.M., Moss, G.F., Neale, M.G., and Ritchie, J.T. (1973). The absorption, metabolism and excretion of disodium cromoglycate in nine animal species. Toxicol. Appl. Pharmacol. 26, 319–328.
45. Smith, D., and Fisher, A. (1989) Age related changes in the clearance and oral absorption of sodium cromoglycate in the developing albino rat. J. Pharm. Pharmacol. 32, 823–827,
46. Cox, J.S.G., Beach, J.E., Blakr, A.M.I.N., Clarke, A.I., King, J., Lee, T.B., Loveday, D.E.E., Moss, G.F., Orr, T.S., Ritchie, J.T., and Sheard, P. (1970). Disodium cromoglicate (Intal). Adv. Drug Res. 5, 115–196.
47. Esposito P., Gheorghe D., Kandere K., Pang X., Connolly R., Jacobson S., and Theoharides, T.C. (2001). Acute stress increases permeability of the blood–brain barrier through activation of brain mast cells. Brain Res. 888, 117–127.
48. Hayashi, T., Cottam, H.B., Chan, M., Jin, G., Tawatao, R.I., Crain, B., Ronacher, L., Messer, K., Carson, D., and Corr, M. (2008). Mast cell-dependent anorexia and hypothermia induced by mucosal activation of Toll-like receptor 7. Am. J. Physiol. Regul. Integr. Comp. Physiol. 295, R123–R132.
49. Nava, F., and Caputi, A. (1999). Central effects of cromoglycate sodium salt in rats treated with lipopolysaccharide. Eur. J. Pharmacol. 367, 351–359.
50. Sakata, T., Ookuma, K., Fukagawa, K., Fujimoto, K., Yoshimatsu, H., Shiraishi, T., and Wada, H. (1988). Blockade of the histamine H1-receptor in the rat ventromedial hypothalamus and feeding elicitation. Brain Res. 441, 403–407.
51. Kharatishvili, I., Nissinen, J.P., McIntosh, T.K., and Pitkänen, A. (2006). A model of posttraumatic epilepsy induced by lateral fluid-percussion brain injury in rats. Neuroscience 140, 685–697.
52. Roe, S.Y., and Rothwell, N.J. (1997). Whole body metabolic responses to brain trauma in the rat. J. Neurotrauma 14, 399–408.
53. Crenn, P., Hamchaoui, S., Bourget-Massari, A., Hanachi, M., Melchior, J.C., and Azouvi, P. (2014). Changes in weight after traumatic brain injury in adult patients: a longitudinal study. Clin. Nutr. 33, 348–353.
54. Walker, W.C., and Pickett, T.C. (2007). Motor impairment after severe traumatic brain injury: a longitudinal multicenter study. J. Rehabil. Res. Dev. 44, 975–982.

55. Hicks, R., Soares, H., Smith, D., and McIntosh, T. (1996). Temporal and spatial characterization of neuronal injury following lateral fluid-percussion brain injury in the rat. Acta Neuropathol. 91, 236–246.
56. Grady, M.S., Charleston, J.A.Y.S., Maris, D.O.N., Witgen, B.M., Lifshitz, J., and Al, G.E.T. (2003). Neuronal and glial cell number in the hippocampus after experimental traumatic brain injury: analysis by stereological estimation. J. Neurotrauma 20, 929–941.
57. Baldwin S.A., Gibson T., Callihan C.T., Sullivan P.G.l., Palmer E., and Scheff S.W. (1997). Neuronal cell loss in the CA3 subfield of the hippocampus following cortical contusion utilizing the optical disector method for cell counting. J. Neurotrauma 14, 385–398.
58. Yasmin A., Pitkänen A., Jokivarsi K., Poutiainen P., Gröhn O., and Immonen R. (2019). MRS reveals chronic inflammation in T2w MRI-negative perilesional cortex - a 6-months multimodal imaging follow-up study. Front. Neurosci. 13, 863.
59. Vuokila N., Das Gupta S., Huusko R., Tohka J., Puhakka N., and Pitkänen A. (2020). Elevated acute plasma miR-124-3p level relates to evolution of larger cortical lesion area after traumatic brain injury. Neuroscience 433, 21–35.
60. Kabadi S.V., Hilton G.D., Stoica B.A., Zapple D.N., and Faden A.I. (2010). Fluid-percussion-induced traumatic brain injury model in rats. Nat. Protoc. 5, 1552–1563.
61. Witgen, B.M., Lifshitz, J., Smith, M.L., Schwarzbach, E., Liang, S.L., Grady M.S., and Cohen, A.S. (2005). Regional hippocampal alteration associated with cognitive deficit following experimental brain injury: a systems, network and cellular evaluation. Neuroscience 133, 1–15.
62. Smith, D.H., Chen, X.H., Pierce, J.E., Wolf, J.A., Trojanowski, J.Q., Graham, D.I., and McIntosh, T.K. (1997). Progressive atrophy and neuron death for one year following brain trauma in the rat. J. Neurotrauma 14, 715–727.
63. Bramlett, H.M., Dietrich, W.D., Green, E.J., and Busto, R. (1997). Chronic histopathological consequences of fluid-percussion brain injury in rats: effects of post-traumatic hypothermia. Acta Neuropathol. 93, 190–199.
64. Statler K.D., Alexander H., Vagni V., Dixon C.E., Clark R.S., Jenkins L., and Kochanek P.M. (2006). Comparison of seven anesthetic agents on outcome after experimental traumatic brain injury in adult, male rats. J. Neurotrauma 23, 97–108.
65. Cortez, S.C., McIntosh, T.K., and Noble L.J. (1989). Experimental fluid percussion brain injury: vascular disruption and neuronal and glial alterations. Brain Res. 482, 271–282.
66. Scheff, S.W., Price, D.A., Hicks, R.R., Baldwin, S.A., Robinson S., and Brackney, C. (2005). Synaptogenesis in the hippocampal CA1 field following traumatic brain injury. J. Neurotrauma 22, 719–732.
67. Gao, X., Deng, P., Xu, Z.C., and Chen, J. (2011). Moderate traumatic brain injury causes acute dendritic and synaptic degeneration in the hippocampal dentate gyrus. PLoS One 6, e24566.
68. Maxwell, W.L., Dhillon, K., Harper, L., Espin, J., McIntosh, T.K., Smith, D.H., and Graham, D.I. (2003). There is differential loss of pyramidal cells from the human hippocampus with survival after blunt head injury. J. Neuropathol. Exp. Neurol. 62, 272–279.
69. Abdel-Salam, O.M., Youness, I.R., Mohammed, N.A., Omara, E.A., Khadrawy, Y.A., and Sleem, A.A. (2016). Neuroprotection by mast cell stabilizers and histamine H1 receptor blockade in rotenone-induced oxidative stress and nigrostriatal damage. React. Oxyg. Species 1, 228–244.
70. Wagstyl, K., and Lerch, J.P. (2018). Cortical thickness, in: *Brain Morphometry.* Spalleta, G., Piras, F., and Gili, T. (eds). Humana Press: New York, pps. 35–49.
71. Racine R., Rose P.A., and Burnham W.M. (1997). After discharge thresholds and kindling rates in dorsal and ventral hippocampus and dentate gyrus. J Neurol Sci. 4, 273–278.
72. Becker A., Letzel K., Letzel U., and Grecksch G. (1997). Kindling of the dorsal and the ventral hippocampus: effects on learning performance in rats. Physiol. Behav. 62, 1265–1271.
73. D'Ambrosio, R., Fender, J.S., Fairbanks, J.P., Simon, E.A., Born, D.E., Doyle, D.L., and Miller, J.W. (2005). Progression from frontal-parietal to mesial-temporal epilepsy after fluid percussion injury in the rat. Brain 128, 174–188.
74. Huttunen, J.K., Airaksinen, A.M., Barba, C., Colicchio, G., Niskanen, J.P., Shatillo, A., Sierra Lopez, A., Ndode-Ekane, X.E., Pitkänen, A., and Gröhn, O.H. (2018). Detection of hyperexcitability by functional magnetic resonance imaging after experimental traumatic brain injury. J. Neurotrauma 35, 2708–2717.
75. Sloviter, R.S. (1994). The functional organization of the hippocampal dentate gyrus and its relevance to the pathogenesis of temporal lobe epilepsy. Ann. Neurol. 35, 640–654.
76. Wenzel, H.J., Woolley, C.S., Robbins, C.A., and Schwartzkroin, P.A. (2000). Kainic acid-induced mossy fiber sprouting and synapse formation in the dentate gyrus of rats. Hippocampus 10, 244–260.
77. Gulyaeva N.V. (2019). Functional neurochemistry of the ventral and dorsal hippocampus: stress, depression, dementia and remote hippocampal damage. Neurochem. Res. 44, 1306–1322.

Address correspondence to:
Luis Concha, MD, PhD
Institute of Neurobiology
National Autonomous University of Mexico
Campus Juriquilla
Queretaro
Mexico

E-mail: lconcha@unam.mx

or

Luisa Rocha, MD, PhD
Department of Pharmacobiology
Center of Research and Advanced Studies
Mexico City
Mexico

E-mail: lrocha@cinvestav.mx